scientific reports

OPEN

Novel sulfonic groups grafted sugarcane bagasse biosorbent for efficient removal of cationic dyes from wastewater

A. I. Abd-Elhamid[1], A. G. Mostafa[2], A. A. Nayl[3] & M. A. Akl[2]✉

In this research, we reported the synthesis of effective sulphonated sugarcane bagasse (SCB@SA) biosorbent based on agriculture waste materials via a simple diazotization strategy for the removal of methylene blue (MB) and Bismarck Brown R(BB) dyes from waste water samples. First, the sugarcane bagasse (SCB) waste was collected, grinded, and sieved to obtain the desired size. Secondly, the SCB powder is modified with sulfanilinic acid (SA) via the formation of its diazonium salt to introduce sulfonic groups on the SCB surface. Different advanced techniques were applied to characterize the prepared materials before and after the adsorption process viz. Scanning electron microscopy (SEM), transmission electron microscopy (TEM), Fourier transform infrared spectroscopy (FTIR), X-ray diffraction (XRD), Energy-dispersive X-ray spectroscopy (EDS) and Thermogravimetric analysis (TGA). Different parameters affecting the adsorption process of both MB and BB were studied. Because of the higher correlation coefficient ($R^2 \geq 0.999$) and lower error functions, the equilibrium MB and BB adsorption isotherms for a single-dye system fit Langmuir with maximum adsorption capacity reaching to 127.48 and 166.75 mg/g for MB and BB, respectively. Moreover, the R_L values obtained for both dyes lie between 0 and 1, indicating that MB and BB adsorption by SCB@SA is a favorable process. Besides, the error functions' values of the pseudo-2nd-order are significantly lower than those of the pseudo-1st-order, implying that the adsorption MB and BB onto SCB@SA biosorbent fitted the pseudo-2nd-order kinetic model in a chemosorption manner. In the thermodynamic studies, the adsorption process is spontaneous, exothermic, and has less randomness. In addition, the SCB@SA biosorbent could be reused in five cycles maintaining on suitable adsorption efficiency. Finally, the MB and BB dyes could be adsorbed on the SCB@SA biosorbent via three mechanisms including π-π stacking, columbic attraction, and hydrogen bonding.

Organically synthesized dyes are required in several industries such as textile, leather, painting, paper, cosmetics, etc[1–3]. The presence of these colored dyes in wastewater has a toxic effect on the surrounding environment as well as the living organism[4,5]. Besides, even at very low concentrations, the colored dyes are easily detected in the water bodies making them undesirable[6]. Moreover, these dyes retard the penetration of sunlight into water which affects the aquatic-organisms.

Thus, it is necessary to treat this wastewater before release into the water body. Several technologies were examined such as physical, chemical, and biological approches. Adsorption among these approaches exhibits easy operation, economic process, simple setup and does not require complicated technology. Numerous adsorbents were employed for such process[7–12] such as commercial active carbon, natural materials, bio-adsorbents, and wastes from agriculture. Agriculture wastes are these portions that are residue from agriculture operations. These unwanted materials are enriched with cellulose, hemicellulose, and lignin which provide several kinds of

[1]Composites and Nanostructured Materials Research Department, Advanced Technology and New Materials Research Institute (ATNMRI), City of Scientific Research and Technological Applications (SRTA-City), New Borg Al-Arab, Alexandria 21934, Egypt. [2]Chemistry Department, Faculty of Science, Mansoura University, Mansoura 35516, Egypt. [3]Department of Chemistry, College of Science, Jouf University, 72341 Sakaka, Aljouf, Saudi Arabia. ✉email: maagdaakl@yahoo.com

functional groups such as ether, alcohols, aldehydes, carboxylic, ketones, and phenolic groups[13]. These oxygenated functional groups possess a tendency to interact with wastewater pollutants. Moreover, they make the biomasses suitable substrate material and able to be modified with various function groups.

The adsorption capacity of the native biomass is still limited towards the water's contaminants. Therefore, several strategies were investigated to improve the affinity of the biomasses towards the dye pollutants. For example, the preparation of amphoteric materials derived from wheat straw (WS)[14]. Initially, WS was soaked in 3% w/w NaOH at 100 °C and then hydrolyzed with 200 ml 4% v/v HCl at 80 °C. Thereafter, the pretreated WS was grafted with mono chloroacetic acid and then anchored polymerized cationic monomer of 2-(dimethylamino) ethyl methacrylate for removal. Peanut husk was functionalized by hexadecylpyridinium bromide (CPB)[15]. In this study peanut husk was collected, washed, crushed, and sieved. Thereafter, the peanut husk powder was reacted with (CPB). Sawdust was grafted with polyaniline[16]. In this study, raw sawdust was smatched, sieved, and alkali treated. Then, the alkali treated sawdust was modified with polyaniline through aniline monomer polymerization using $FeCl_3$ as an oxidant at room temperature. Biosorbent hybrid material wood modified with residue aluminum oxide was investigated by Velinov et al.[17]. Ghosh and Bandyopadhyay collected woodchips (oak trees) with lignocellulosic structures wasted from wood industries, fractionated by sieve, treated with acid and alkali, and finally loaded with Al_2O_3. Bamboo leaves were modified using citric acid [18], in which bamboo leaves were collected, cleaned, grinded, and sieved using 120 mesh and thermally treated at 450 °C for 6 h. After that, the carbonized material was sonicated with citric acid to yield the adsorbent. Moringa oleifera leaf was modified with H_3PO_4 by Bello et al[19]. Here, moringa seed pod was grounded and sieved to a size of 106 μm followed by mixing with 0.3 mol/dm³ H_3PO_4. The mixture was stirred and heated to form a paste; this paste was thermally treated at 300 °C for 30 min.

The dediazonation of diazonium salts is an effective strategy for the formation of thin organic films onto various substrates[20]. In which an aryl radical that covalently bonded to the surface leads to graft the desired groups on the substrate.

To the best of our knowledge, SCB modification using a sulfanilinic diazonium salt has not been reported in the literature.

In the present research, we use the sugarcane bagasse waste (zero value, zero cost, environmental contaminante) to prepare a valuable, efficient SCB@SA biosorbent for the removal of toxic cationic dyes from wastewater. The sugarcane bagasse waste was collected, cut, and grinded to the desired size. The obtained powder was then stirred in distilled water for 2 h, filtered, and air dried. Thereafter, we applied dediazonation method to graft sulfanilic acid on the surface of treated sugarcane bagasse waste materials. As a result, reactive sulfonic groups were created on the SCB surface. Different characterization techniques were employed to analyze the prepared materials. Moreover, the sulfonated SCB(SCB@SA) biosorbent was used to remove cationic dyes (MB and BB) from aqueous solutions.

Experimental
Chemicals
The raw SCB waste was collected from the local market. Sodium nitrite($NaNO_2$) (Iso-Chem. High pure grade), sulfanilic acid (Merk, 98%), sodium bicarbonate (Merk, 99%), HCl (Sigma-Aldrich, Lab grade), NaOH (Sigma-Aldrich, Lab grade), Methylene blue (Sigma-Aldrich) and BB (Merck).
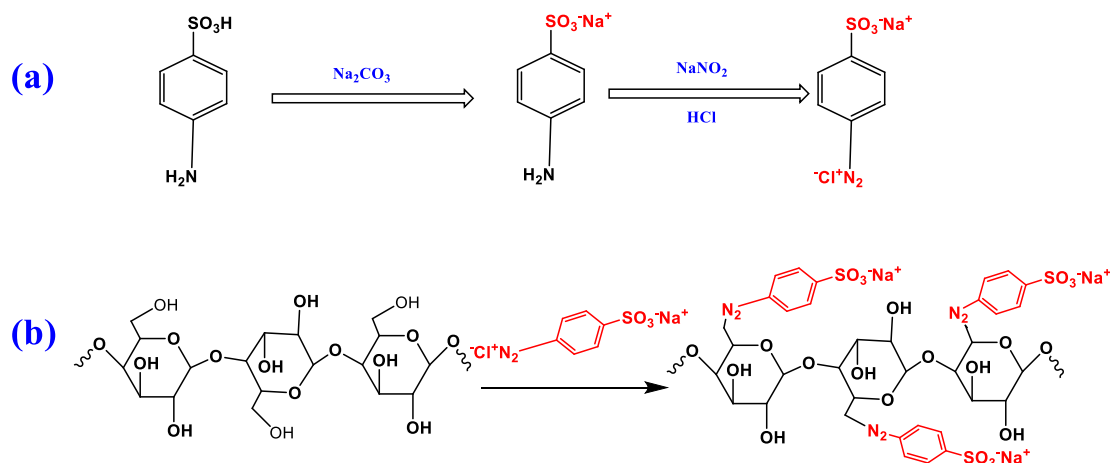
Preparation of SCB
The SCB was prepared as previously reported[21]. Briefly, the raw SCB waste was collected, cut, and grinded to the desired size. The obtained powder was then stirred in distilled water for 2 h, filtered, and air dried.

Preparation of sulphonated sugarcane bagasse (SCB@SA) biosorbent
The SCB@SA was prepared by reacting SCB and sulfanilic diazonium salt. Initially, sulfanilic diazonium salt was prepared by adding 3.4 g sulfanilic acid and 2 g sodium bicarbonate to 50 mL bidistilled water and stirring for complete dissolution. Thereafter, 3 g $NaNO_2$ was added to the previous solution under stirring in an ice bath. Then, a cold concentrated HCl was added to the previous solution and slowly stirred in an ice bath for 3 h to form diazonium salt. 2.3 g SCB was charged to the diazonium solution and stirred for another 2 h in an ice bath to form SCB@SA biosorbent. The obtained solid was washed with distilled water several times to remove unreacted species, dried, and stored for further use. The subsequent steps of preparation of sulfanilic diazonium salt and SCB@SA biosorbent are represented in Fig. 1.

Adsorption experiments
A stock solution of 1000 mg L⁻¹ of each investigated dye was prepared by dissolving the dye powder in distilled water and diluting them as needed. The adsorption experiments of the investigated dyes (MB and BB) were carried out in 125 mL stoppered bottles that contained 10 mL of cationic dye solution and biosorbent SCB@SA dose (0.0075 g). Then, these bottles were shaken at a constant speed of 150 rpm on a thermostat shaker at room temperature (25 °C). After the equilibrium was reached, the solutions were centrifuged at 3000 rpm. The supernatant solution, which includes the remains of the investigated dyes, was measured at the specific at $\lambda_{max} = 662$ nm for MB dye and 465 nm for BB. Various parameters were studied such as contact time (15–240 min), temperature (25–45 °C), SCB@SA adsorbent dose (0.0025–0.02 g), pH from (3.0 to 11.0) for MB and from (2.0 to 8.0) for BB, and initial concentration of dye (50–400 mg L⁻¹). The investigated dye removal percentage (R, %) and adsorption capacity (q_e, mg g⁻¹) were determined as present in Eqs. (1) and (2), respectively[22].

Figure 1. Preparation of **(a)** sulfanilic diazonium salt and **(b)** SCB@SA biosorbent.

$$R\% = \frac{C_i - C_f}{C_i} \times 100 \tag{1}$$

$$qe = \frac{(C_i - C_f) \times V}{wt} \times 100 \tag{2}$$

where, C_i (ppm) and C_f (ppm) are the initial investigated dye concentration and equilibrium dye concentration, respectively. v (L), is the volume of investigated dye, and wt (g) is the SCB@SA dose.

For adsorption of dyes in the binary system, MB and BB dyes were mixed by a ratio of 2:3, respectively. The adsorption experiments of the investigated binary system were performed in 125 ml stoppered bottles that contained 10 ml of cationic mixed dyes' solution and SCB@SA dose (0.0075 g) at pH 7.0 and different time intervals. Followed by shaking at a constant speed of 150 rpm at 25 °C.

Estimation of pHpzc of SCB@SA biosorbent
0.01 M NaCl solution (50 mL) were placed into different 250 mL Erlenmeyer flasks with the initial pH adjusted between 2 and 10 by addition of HCl and/or NaOH (0.1 M).

SCB@SA (0.2 g) was added to each flask and the suspensions were left to stand for 48 h. They were, then, centrifuged, and the final pHfs of the solutions were determined. The pHpzc corresponds to the point where pH 0 in the plot of pHi vs. ΔpH (ΔpH = pH$_i$ − pH$_f$).

Desorption and regeneration investigation
After the adsorption of MB and BB dyes by SCB@SA biosorbent, desorption of the investigated dyes was examined by different eluents including ethanol, NaOH (0.1 mol/L), and sod. bicarbonate (1 mol/L), Na$_2$CO$_3$ (1 mol/L), and HCl (0.1 mol/L). The regeneration of SCB@SA biosorbent was examined through five repeated cycles of adsorption–desorption by the batch method. 0.0075 g of SCB@SA was shaken with 10 ml of 100 ppm for MB and 150 ppm for BB for 120 min; then adsorbent was filtered and then it was eluted with NaOH (0.1 mol/L) and these procedures were repeated for another 4 cycles. The desorption percentage of the investigated cationic dyes (D, %) by SCB@SA was calculated from Eq. (3)[23].

$$D(\%) = \frac{amount\ of\ dye\ desorbed\ to\ the\ solution\ (mg/l)}{amount\ of\ dye\ adsorbed\ on\ SCB@SA\ (mg/l)} \times 100 \tag{3}$$

Results and discussion
Characterizations
SEM and TEM
The surface morphology of the modified SCB (SCB@SA) was detected by employing the SEM, as seen in Fig. 2. At low magnification, the SCB@SA appears as large disordered particles(Fig. 2a, b). With further increases in the magnification (250 X) these particles appeared as pleated seams collected together to form the SCB@SA particles. At high magnification (500×) these seams become more clear, Fig. 2c. This surface morphology would provide a suitable surface area for an efficient adsorption process. The TEM images of SCB@SA captured at different magnifications (2 μm, 1 μm, and 200 nm), Fig. 2d, showed that the SCB@SA has a layered structure and many windings which exposed the binding sites efficiently to the pollutants.
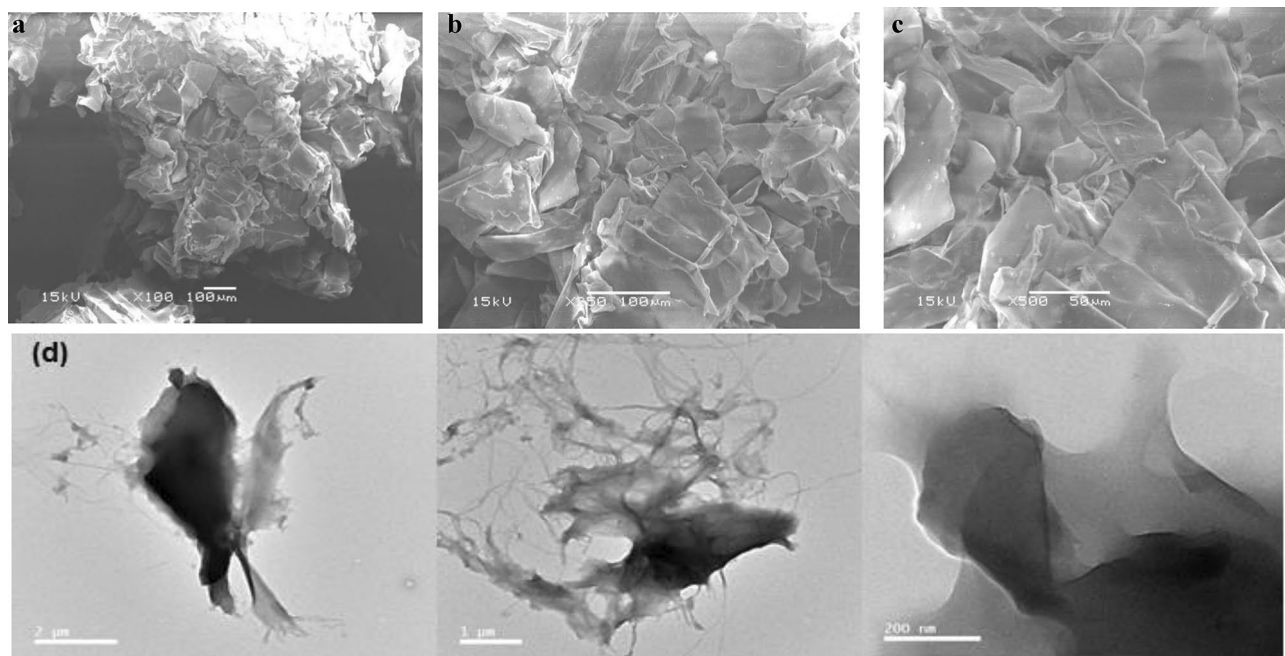
Figure 2. SCB@SA SEM images at different magnifications **(a)** ×100, **(b)** ×250, **(c)** ×500, and **(d)** SCB@SA TEM images at different scales.
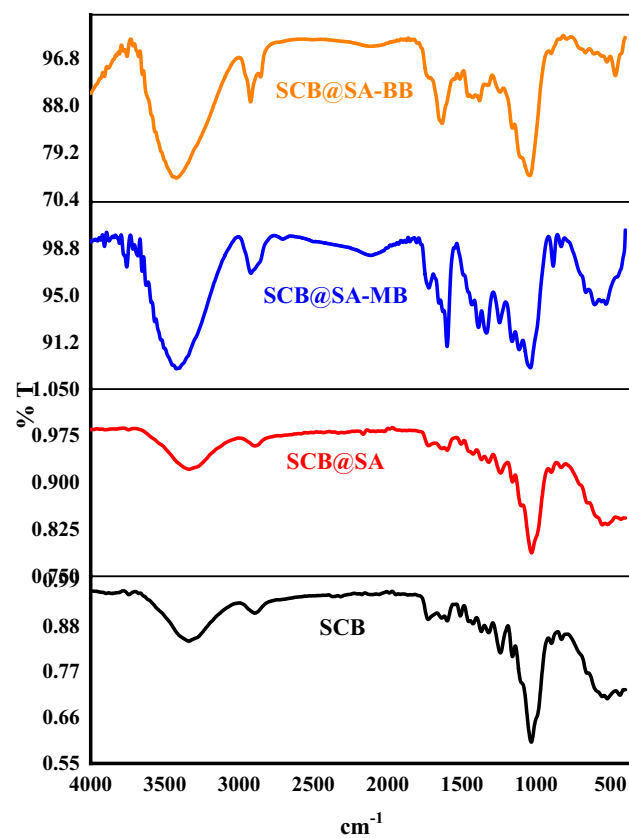
Figure 3. FTIR spectra of SCB, SCB@SA, SCB@SA-MB and SCB@SA-BB.

FTIR

The FTIR analysis of SCB, SCB@SA, SCB@SA-MB, and SCB@SA-BB was carried out as shown in Fig. 3. SCB showed characteristic bands at 3338 cm^{-1} corresponding to absorbed water, 2895 cm^{-1} related to C–H stretching, 1728 cm^{-1} related to COOH groups, 1599 cm^{-1} due to water molecule bending and 1033 cm^{-1} because of C–O stretching. Upon reacting of SCB with diazonium salt to form SCB@SA, the previous bands had small shifts due to the modification process. Moreover, upon adsorption of MB and BB onto SCB@SA biosorbent, the resulting FTIR spectra were highly altered compared to the spectrum of SCB@SA as shown in Fig. 3. These observed results suggested successful adsorption of the dyes on the surface of the used SCB@SA biosorbent.

XRD

The XRD pattern of the raw SCB shows characteristic wide weak peaks at 2θ ≈ 16° and 22°. After modification with sulfanilic acid the intensities and sharpness of these peaks are enhanced, Fig. 4. Besides, another intense peak at 2θ ≈ 28° and other weak peaks at 2θ ≈ 35°, 38°, 42° and 47° also appeared. These observations cleared the enhancement of the crystallinity due to modification with organic material. These findings are in good agreement with the results reported in the literature[24,25].

TGA

The TGA patterns of the raw SCB and SCB@SA biosorbent are shown in Fig. 5. The TGA pattern of the raw SCB showed four main pyrolysis stages; (31–58 °C, 5.20%) due to evaporation of surface water, (58–259 °C, 3.37%) attributed to liberation of interlayer water, the main decomposition stage (259–358 °C, 70.72%) due to degradation of cellulosic chains and finally, (259–358 °C, 16.00%) related to residue carbonization. By modification of SCB with the SA, the amount of absorbed surface water was enhanced by 11% and evaporated at a high temperature of 99 °C which is higher than that of raw SCB. Moreover, the degradation percentage was highly reduced from 70.72 to 52% which provides suitable thermal stability. Finally, the last stage showed an increase in the pyrolysis percentage from 16.00 to 29.00%.

EDS

Figure 6 shows the EDS of SCB and SCB@SA biosorbent. The EDS analysis is required to determine different elemental analyses that compose the analyzed materials. Here, the EDS analysis of SCB mainly consists of C and O-atoms. Moreover, after modification of SCB with diazonium salt, new elements appeared in the EDS analysis of SCB@SA biosorbent such as S and Na-atoms which are related to the anilinic acid.

Adsorption studies

Firstly, we applied unmodified SCB and diazonium-modified material(SCB@SA) for the adsorption of MB and BB, under similar environmental conditions such as the temperature, initial concentration of MB, pH, and the adsorbent dose. As seen in Fig. 7., the diazonium-modified materials showed enhancement in the adsorption efficiency towards MB and BB compared to the original materials. Therefore, further experiments applied the modified SCB@SA biosorbent for studying the optimum adsorption parameters.
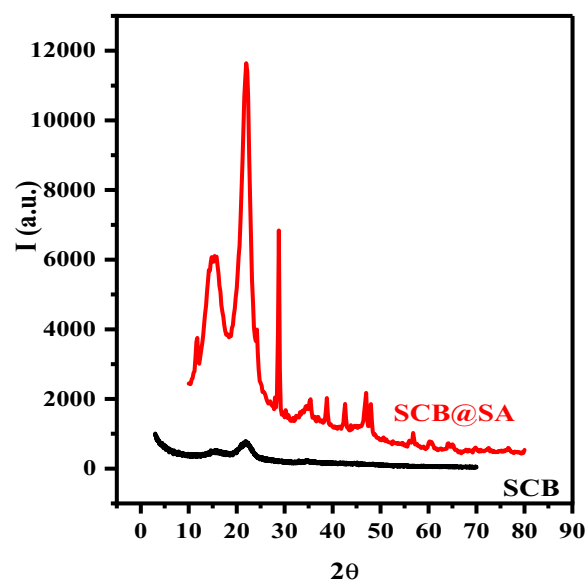
Figure 4. XRD patterns of raw SCB and SCB@SA biosorbent.
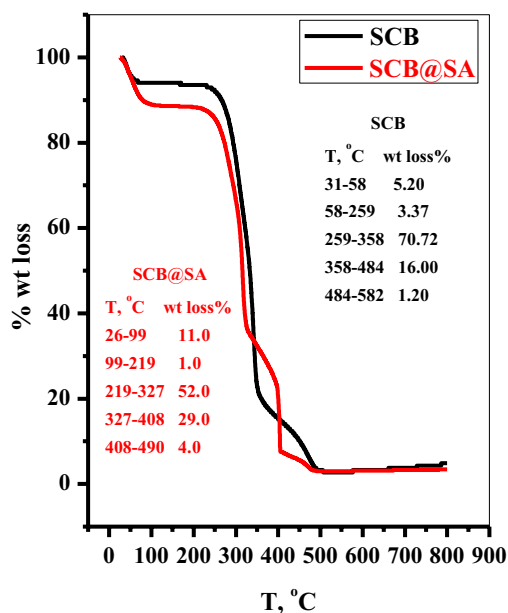
Figure 5. TGA of SCB and SCB@SA.

Effect of pH

The pH of the solution primarily affects the degree of ionization of the dyes and the surface properties of the adsorbents.

The impact of pH on the removal efficiency of MB and BB onto SCB@SA biosorbent was investigated as shown in Fig. 8a. It is clearly noted that the adsorption performance of SCB@SA biosorbent is enhanced with an increase in the solution pH value in the range 2–8. This behavior can be explained as follows: in the acidic environment the density of H⁺ ion in the solution is high; therefore, H⁺ ions will compete with the cationic dye species for the binding sites. By increasing the pH value, the H⁺ ions' density will be reduced and the binding sites will be more ionized ($-SO_3^-Na^+$)[26]. This environment will favour the adsorption of the cationic species. At pH below pHpzc (6.60), Fig. 8b, the surface of SCB@SA biosorbent was positively charged and the adsorption of cationic dyes is decreased due to the repulsive forces. At pH > pHpzc, the surface of SCB@SA biosorbent acquired negative charges resulting in increased adsorption due to greater electrostatic attraction.

Effect of initial dye concentration and adsorption isotherms

In order to study the effect of initial dye concentration on the removal efficiency, the experiments were carried out at various dye concentrations in the range of 50–400 mg/L at room temperature. It was observed that, the removal efficiency significantly decreased from 99 to 24% and from 99 to 32% for MB and BB, respectively upon increase of the dye concentration in the studied range, Fig. 9a. This phenomenon can be explained as follow: at a low initial concentration of the dye, the number of the dye's molecules is well fitted with the number of the binding sites on the adsorbent's surface which results in an improvement of the removal efficiency. With the increase in the initial dye concentration, the number of the dye's molecules will be increased compared to the limited number of the binding sites leading to a decrease in the dye's removal efficiency[27].

For describing the mechanism of the adsorption, Langmuir and Freundlich isotherm models were employed to describe whether adsorption proceeded on a homogeneous or heterogeneous active site's surface. Langmuir, and Freundlich's isothermal models, which can indicate the maximum adsorption capacity (q_e) and binding affinity, were applied in the linear form and the parameters were determined as present in Eqs. (4), (5), and (6), respectively. The dimensionless equilibrium factor (R_L) presented in Eq. (7), is an important parameter that is used in adsorbent-sorbate affinity prediction. Its values are explained as follows: if the R_L value is found to be greater than 1.0 this means that the investigated material is unsuitable and unfavorable, while if it is found to be ($0 < R_L < 1$), ($R_L = 0$), or ($R_L = 1$) this means the reaction is favorable, irreversible, or linear, respectively The Langmuir and Freundlich isotherm model that can be expressed by equations[1]:

$$\ln q_e = \ln q_m - k\varepsilon^2 \tag{4}$$

$$\frac{C_e}{q_e} = \frac{1}{k_L q_m} + \frac{C_e}{q_m} \tag{5}$$

$$\ln q_e = \ln K_f + \frac{1}{n} \ln C_e \tag{6}$$
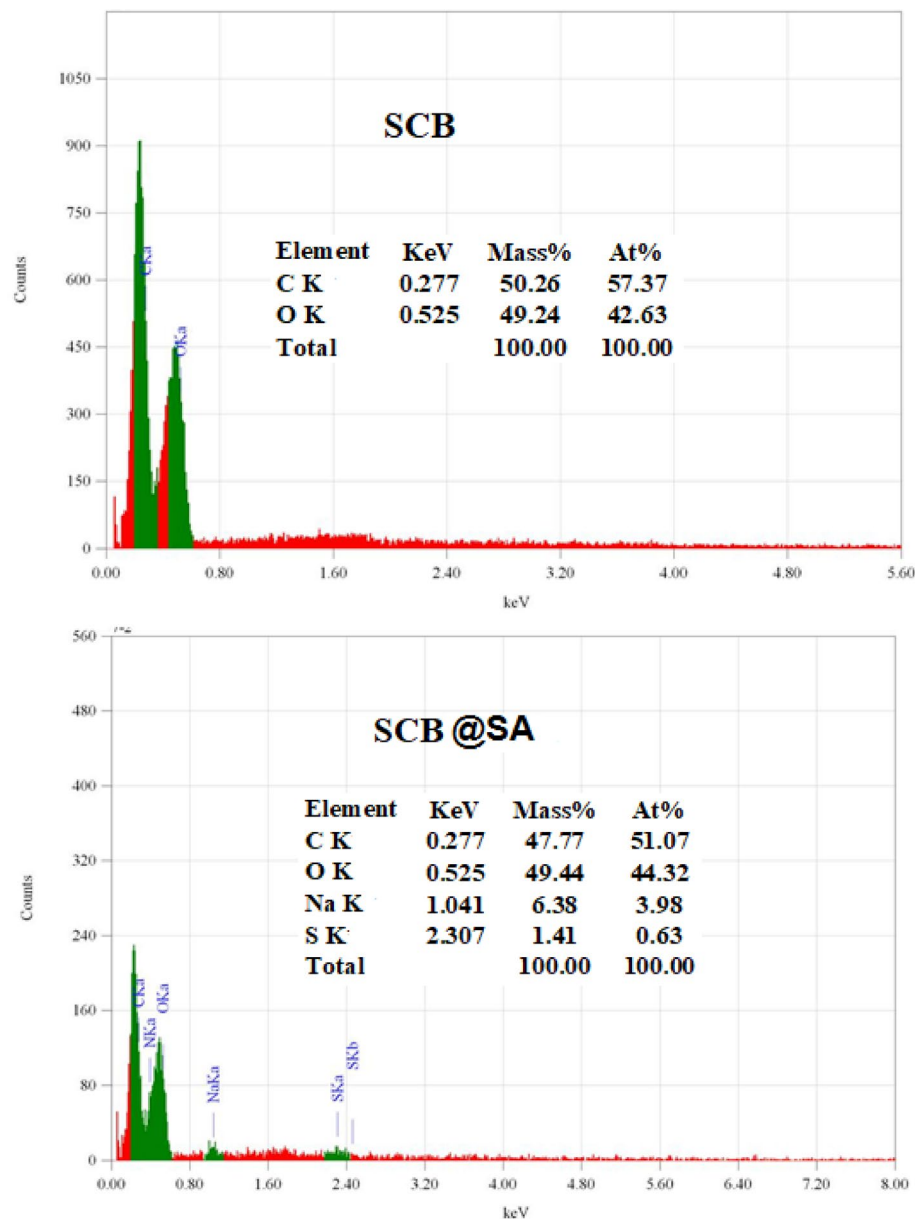
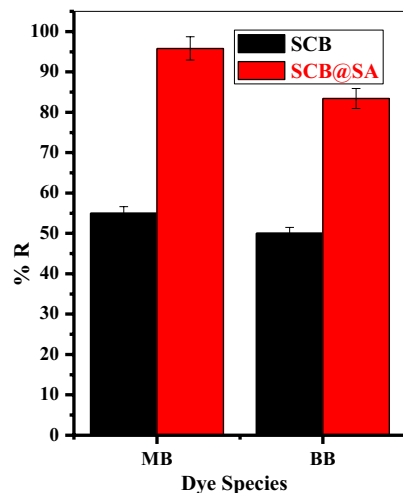**Figure 6.** EDS of raw SCB and SCB@SA biosorbent.

$$R_l = \frac{1}{1 + K_l C_\circ} \tag{7}$$

### Estimation of the best fitted isotherm models

Many error functions were employed to investigate the well-fitted kinetic and isotherm models and also to decrease the error distribution between the calculated values from theoretical model correlations and experimental data. Four error functions were utilized including chi-square statistic (χ^2), mean square error (MSE), the sum of squares error (SSE), and hybrid fractional error (HYBRID). that are presented in Eqs. (8)–(11), respectively[28,29].

$$\chi^2 = \sum_{i=1}^{n} \frac{(q_{ei}exp - q_{ei}cal)^2}{q_{ei}exp} \tag{8}$$

$$MSE = \frac{1}{N_{exp}} \sum_{i=1}^{n} (q_{ei}exp - q_{ei}cal)^2 \tag{9}$$

Figure 7. Comparison between the removal percentage (R%) of MB and BB using raw SCB and SCB@ SA biosorbent.
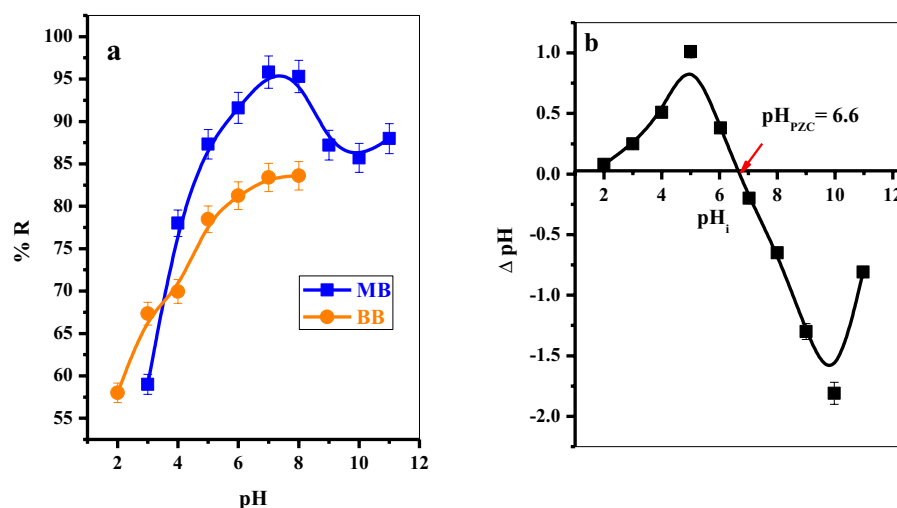
Figure 8. (**a**) pH effect on MB and BB adsorption efficiency onto SCB@SA (T = 25 °C, dose = 0.0075 g, [MB] = [BB] = 100 mg/L; v = 10 mL), (**b**) The pH_{pcz} of SCB@SA biosorbent.

$$SSE = \sum_{i=1}^{n} (q_{ei}exp - q_{ei}\text{cal})^2 \tag{10}$$

$$HYBRID = \frac{100}{N_{exp} - N_{parameter}} \sum_{i=1}^{n} \frac{q_{ei}exp - q_{ei}\text{cal}}{q_{ei}exp} \tag{11}$$

where, n is the number of included observations. The subscript *cal* refers to theoretically calculated data while *exp* subscript represent experimental data.

Table 1 provides the fitted parameter values for the adsorption isotherm models. Because of the higher correlation coefficient ($R^2 \geq 0.999$) and the lower error functions, the equilibrium adsorption isotherms of MB and BB for a single-dye system fit Langmuir isotherm model. This indicated that Langmuir isotherm fitted well the experimental data for both the two-model dye and both dyes prefer to adsorb on the adsorbent as monolayer on equally energetic binding sites. Moreover, the R_L values obtained for both dyes lie between 0 and 1, indicating that MB and BB adsorption by SCB@SA biosorbent is a favorable process.

*Effect of shaking time and kinetic studies*
The effect of the shaking time on the removal efficiency of MB and BB dyes was investigated and plotted in Fig. 10a. We observed that the removal efficiency markedly increased with further passage of the time till it reached equilibrium at 120 min. Thereafter, the removal efficiency attained a constant curve with a further
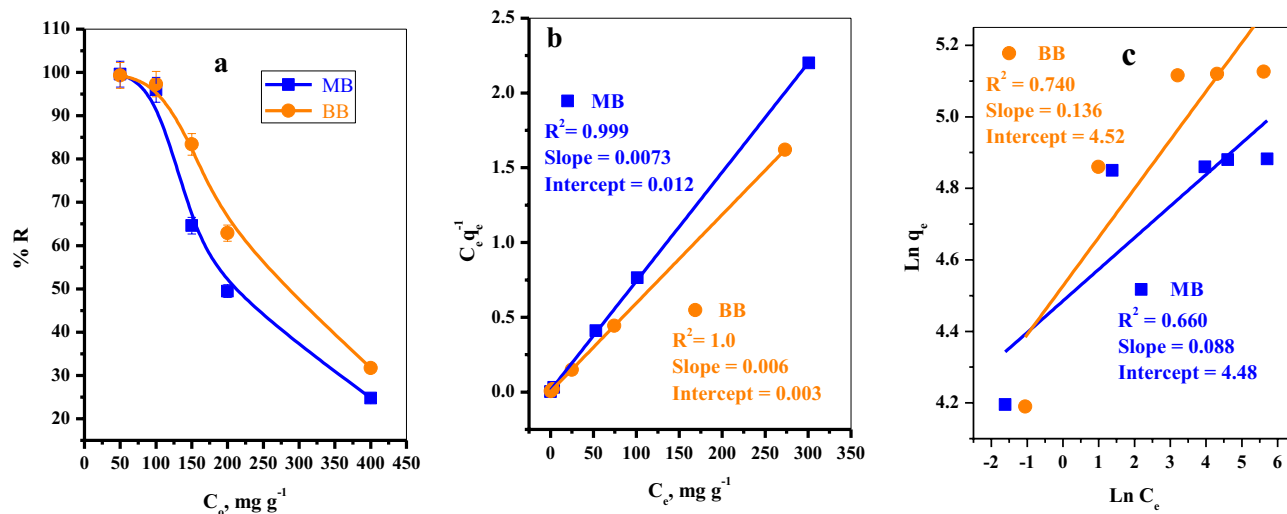
Figure 9. (a) Effect of initial concentration of MB and BB on the removal percentage (**b**) Langmuir isotherm model, (**c**) Freundlich isotherm model for MB and BB adsorption.

Dye	Isotherm model	Parameters	
MB	Langmuir isotherm model	q_e(mg/g)	136.99
		b (l/mg)	0.466
		R_L	0.021
		R^2	0.999
		χ^2	76.52
		SSE	5174.14
		MSE	1034.83
		HYBRID	31.731
	Freundlich isotherm model	1/n	0.088
		K_f (mg/g)	0.221
		R^2	0.740
		χ^2	93.27
		SSE	7914.28
		MSE	1582.856
		HYBRID	14.431
BB	Langmuir isotherm model	Q(mg/g)	166.67
		b (l/mg)	2
		R_L	0.0033
		R^2	1.00
		χ^2	164.13
		SSE	11,520.81
		MSE	2304.163
		HYBRID	44.875
	Freundlich isotherm model	1/n	0.136
		K_f (mg/g)	0.223
		R^2	0.660
		χ^2	224.73
		SSE	16,486.7
		MSE	3297.3
		HYBRID	59.65

Table 1. Langmuir and Freundlich isotherm models for SCB@SA-MB and SCB@SA-BB.
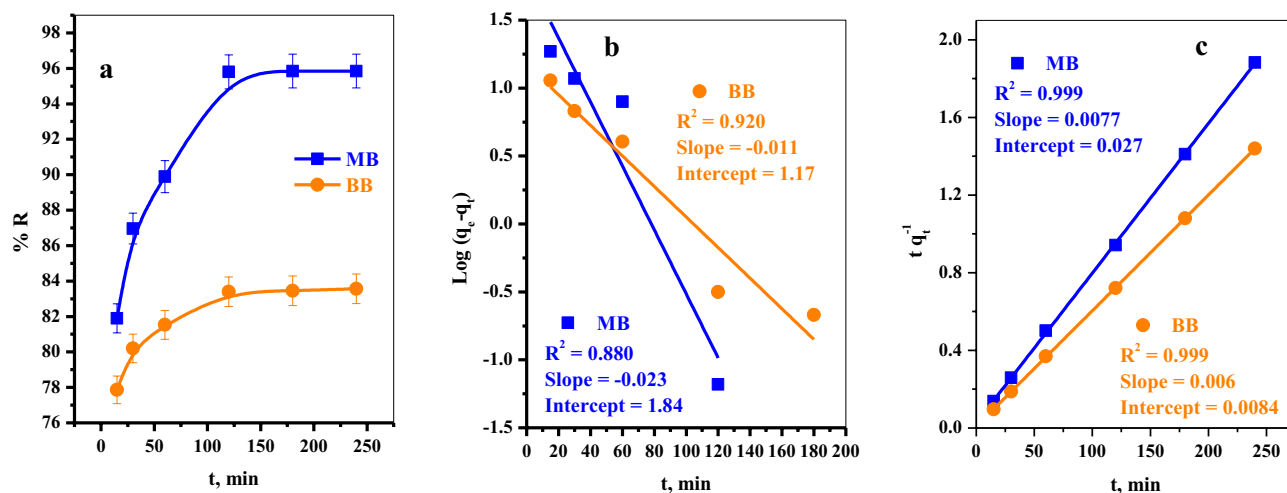
Figure 10. (**a**) Effect of shaking time on the removal percentage of MB and BB using SCB@SA biosorbent, (**b**) Pseudo-1st-order for MB and BB adsorption, and (**c**) pseudo-2nd-order for MB and BB adsorption onto SCB@SA biosorbent.

increase in the shaking time. The rapid adsorption kinetics denotes strong surface complexation among the dye species and sulfonated binding sites[30].

The kinetic behavior and adsorption mechanism can be analyzed by applying the adsorption kinetic models (pseudo-first-order and pseudo-second-order) to demonstrate the experimental data. The linear formulas of pseudo-first order and pseudo-second order are presented in Eqs. (12) and (13), respectively.

The kinetic parameters obtained from the slope and intercept (Fig. 10b, c) were calculated and listed in Table 2. The correlation coefficients ($R^2 = 0.999$) cross-ponding to the pseudo-second-order for both studied dyes are larger than those for the pseudo-first-order. Moreover, the calculated values of adsorption capacities for both two dyes are highly close to those obtained from experiments. This proved that the pseudo-second order kinetics model was fitted with experimental data.. Besides, the error functions' values of the pseudo-2nd-order are significantly lower than those of the pseudo-1st-order, implying that the adsorption of MB and BB onto SCB@SA biosorbent fits the pseudo-2nd-order kinetic model in a chemosorption manner[28].

$$\log(q_e - q_t) = \log q_e + \frac{K_{ads}t}{2.303} \tag{12}$$

$$\frac{t}{q_t} = \frac{1}{K_2 q_e^2} + \frac{t}{q_e} \tag{13}$$

Effect of biosorbent dose

The effect of an biosorbent dose (2.5–20 mg) on the removal efficiency of MB and BB was studied as shown in Fig. 11. It was clearly noted that the adsorption performance of both MB and BB dyes was improved with the increase in the amount of biosorbent used in range (2.5 to 7.5 mg). Thereafter, the adsorption percent remained constant with a further increase in the dose to 20 mg. In this situation, with increase in the adsorbent dose, the number of binding sites is increased . As a result, the removal of both studied dyes were enhanced till the number of binding sites fitted the number of the dye species[31]. Thereafter, any further increase in the adsorbent dose will not show an increase in the adsorption efficiency.

Effect of temperature and thermodynamic studies

The adsorption process is generally impacted by the solution's temperature. Here, the effect of solution's temperature in the range (25–45 °C) on the adsorption efficiency of MB and BB dye is presented in Fig. 12a. We observed that the adsorption percent is declined with a further increase in the temperature above 25 °C. This decrease can be attributed to the increase in the adsorption solution's temperature, which leads to a reduction in the thickness of the boundary layer, due to the high tendency of the dye species to emit from the adsorbent surface to the solution phase, as a result the adsorption efficiency decrease[32].

The thermodynamic factors such as Gibbs free energy change ΔG^o (J mol^{-1}), enthalpy change ΔH^o (J mol^{-1}) and entropy change ΔS^o (J mol^{-1} K^{-1}) were measured employing the equations:

$$\Delta G^o = -RTLnK \tag{14}$$

$$LnK = \frac{\Delta S^o}{R} - \frac{\Delta H^o}{RT} \tag{15}$$

where R is the universal gas constant (8.314 J/mol K) and T is temperature (K).

Dye	$q_{e\ exp}$ (mg/g)	Kinetic model	Parameters	
MB	127.48	First-order kinetic model	K_1 (min^{-1})	⁻0.053
			q_e	69.2
			R^2	0.880
			χ^2	134.3
			SSE	16,464.2
			MSE	2744
			HYBRID	51.193
		Second-order kinetic model	K_2 (g mg^{-1} min^{-1})	0.0022
			$q_{e\ cal}$ (mg/g)	129.87
			R^2	0.999
			χ^2	107.9
			SSE	12,772.4
			MSE	2128.7
			HYBRID	45.772
BB	166.75	First-order kinetic model	K_1 (min^{-1})	⁻0.025
			q_e	14.8
			R^2	0.920
			χ^2	808.1
			SSE	131,769.4
			MSE	21,961.57
			HYBRID	109.1
		Second-order kinetic model	K_2 (g mg^{-1} min^{-1})	0.0043
			$q_{e\ cal}$ (mg/g)	166.67
			R^2	0.999
			χ^2	1.21
			SSE	189.4
			MSE	31.57
			HYBRID	2.841

Table 2. Pseudo-first-order and pseudo-second-order kinetic model parameters for adsorption of MB and BB-dye from aqueous solution.
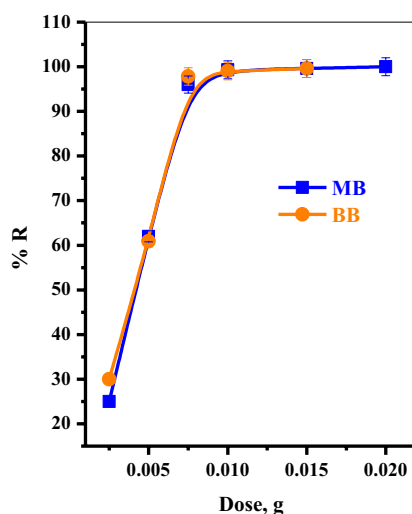
Figure 11. Effect of biosorbent dose on MB and BB removal percentage.

The values of ΔHº and ΔSº were calculated from the slope and intercept from Fig. 12b and are listed in Table 3. As can be seen, the estimated negative ΔGº values prove that the MB and BB adsorption on SCB@SA biosorbent is spontaneous in addition to the thermodynamic feasibility of the MB and BB adsorption under the investigated temperature range. Moreover, the ΔHº negative charge indicates that the MB and BB adsorption process was
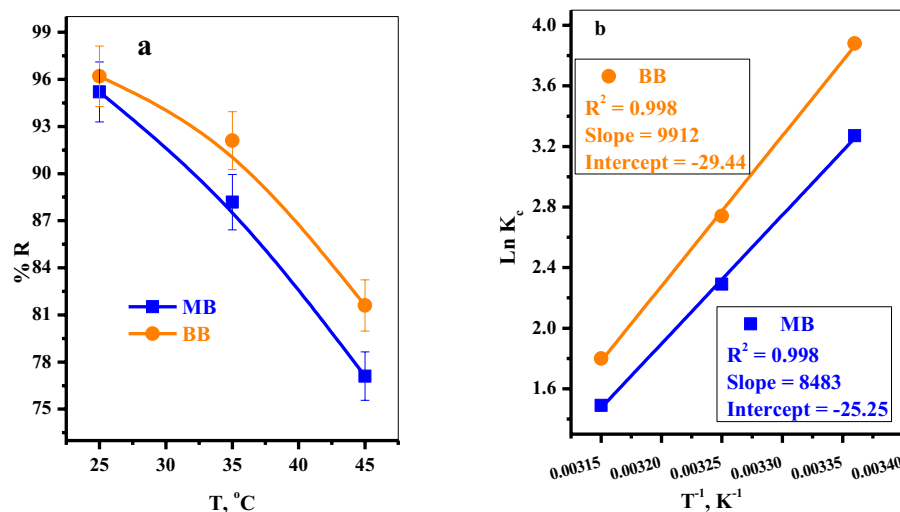
Figure 12. (a) Effect of temperature on MB and BB removal percentage and (b) Plot of ln K_C versus (1/T) absolute temperature for the adsorption of MB and BB on the SCB@SA surface.

System	Kc			ΔG^o (KJ /mol)			ΔH^o (KJ/mol)	ΔS^o (J/mol K)
	298 K	308 K	318 K	298 K	308 K	318 K		
MB	26.375	9.92	4.48	−8.1	−5.874	−3.9658	−71.6	−213.17
BB	48.42	15.48	6.04	−9.61	−7.016	−4.758	−82.411	−244.76

Table 3. Thermodynamic parameters for adsorption of MB and MB using SCB@SA biosorbent.

exothermic. Besides, the -ve charge of the ΔS^o signifies that MB and BB adsorption results in lower randomness and alignment increase. It was noticed that the adsorption of MB and BB is decreased as the temperature increases[1].

Desorption/reusability studies
In order to investigated the reusability of SCB@SA biosorbent, 5 cycles of MB and BB adsorption–desorption were carried out at the optimum conditions. Several eluents were investigated and it was found that NaOH (0.1 mol/L) is the best among them. Figure 13 shows the obtained data of the repeated five cycles of MB and BB adsorption–desorption using NaOH (0.1 mol/L) as eluent.

### Removal of BB and MB in binary system
Figure 14 represents the removal of BB and MB dyes in the binary system. It was observed that two distinct characteristic peaks for BB and MB clearly appeared at wavelength 475 nm and 666 nm, respectively. As the organic pollutants (dyes) are not present in real polluted water in individual forms, it is very necessary to apply the SCB@SA biosorbent for potential removal of the investigated dyes in the binary system at different time intervals. For the adsorption experiment, 0.0075 g of SCB@SA biosorbent was added to the binary system solution (75 ppm BB and 50 ppm MB) at pH 7. Then the mixture was shaken at 150 rpm. The equilibrium concentration of the adsorbates was calculated from UV–Vis data. The adsorption efficiency of BB and MB was calculated by employing Eq. (2). As it can be noticed from Fig.14, the absorbance, which is an indication of the dye's concentration, is markedly reduced with increasing time of adsorption denoting the efficient use of SCB@SA biosorbent for the removal of the investigated dyes in the binary system.

Plausible mechanism of adsorption
The adsorption mechanism of MB and BB onto the SCB@SA biosorbent was expected by taking into consideration the SO_3^- functional groups on the SCB@SA surface. In a pH basic medium, the SCB@SA adsorbs MB and BB via electrostatic interactions between the negatively charged oxygen on the SCB@SA biosorbent and the positively charged groups of the positively charged dyes, as illustrated in Fig. 15. Also, hydrogen bonding had a vital role in the MB and BB adsorption process via the interaction between the SCB@SA hydrogen atoms and nitrogen atoms in the structure of the MB and BB. Additionally, the adsorption of MB and BB can be attributed to the n–π and π–π interactions. The –π-π interactions occurred through the interaction of the aromatic rings of SCB@SA biosorbent with the aromatic rings of MB and BB dyes. While the n–π interactions occurred by the electron-donating groups (the nitrogen and oxygen groups of the SCB@SA) biosorbent interacting with the aromatic rings of MB and BB.
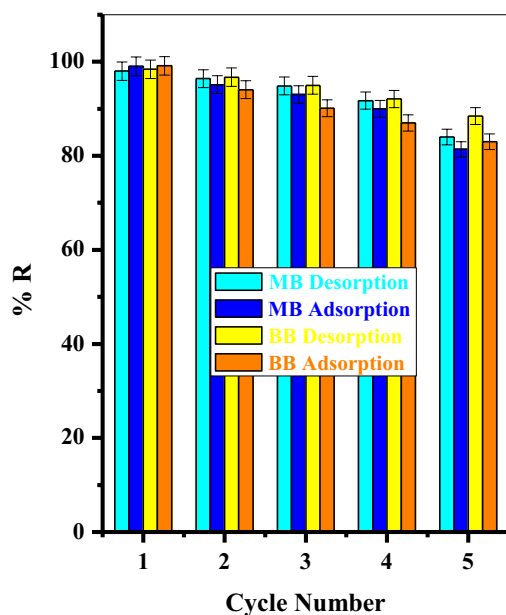
**Figure 13.** Repeated 5 cycles of MB and BB adsorption–desorption.
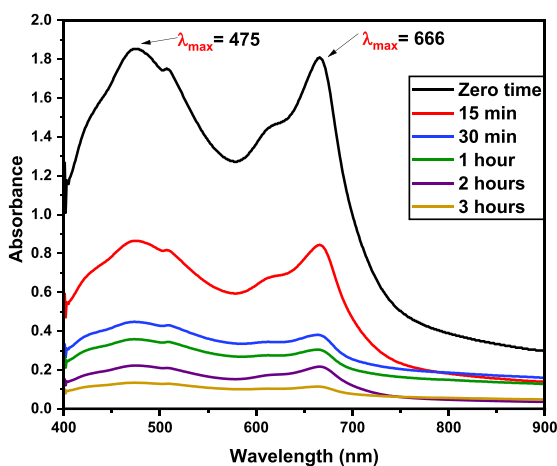
Figure 14. UV data of BB and MB mix after adsorption by SCB@SA at different time intervals.

Performance of SCB@SA biosorbent

Table 4 represents a comparison between the SCB@SA biosorbent performances with other cited adsorbents for remediation of MB and BB taking the sorption capacity, pH and time of adsorption into consideration. Eventually, the SCB@SA biosorbent has high capacities and efficiencies for both MB and BB recovery compared to other mentioned adsorbents as found in Table 4.

Conclusion

In this work, we successfully functionalized SCB, as a low-cost material, with the sulfonic groups using a simple dediazonation route. The as-prepared material SCB@SA biosorbent was employed for the removal of MB and BB dyes from the aqueous solutions. Different techniques such as SEM, TEM, FTIR, EDS, XRD, and TGA have been performed to characterize the synthesized materials. The higher R^2 values and the lower error functions suggested that the adsorption process obeyed the pseudo-second-order kinetic model and Langmuir isotherm with maximum adsorption capacities of 127.48 and 166.75 mg/g for MB and BB, respectively. Moreover, the SCB@SA biosorbent can be regenerated several times with suitable adsorption efficiency after 5 cycles. The plausible mechanism of adsorption of the investigated cationic dyes onto SCB@SA, was elucidated. The process of fabrication, and characterization and application of SCB@SA in cationic dyes' remediation is graphically presented in Fig. 16.
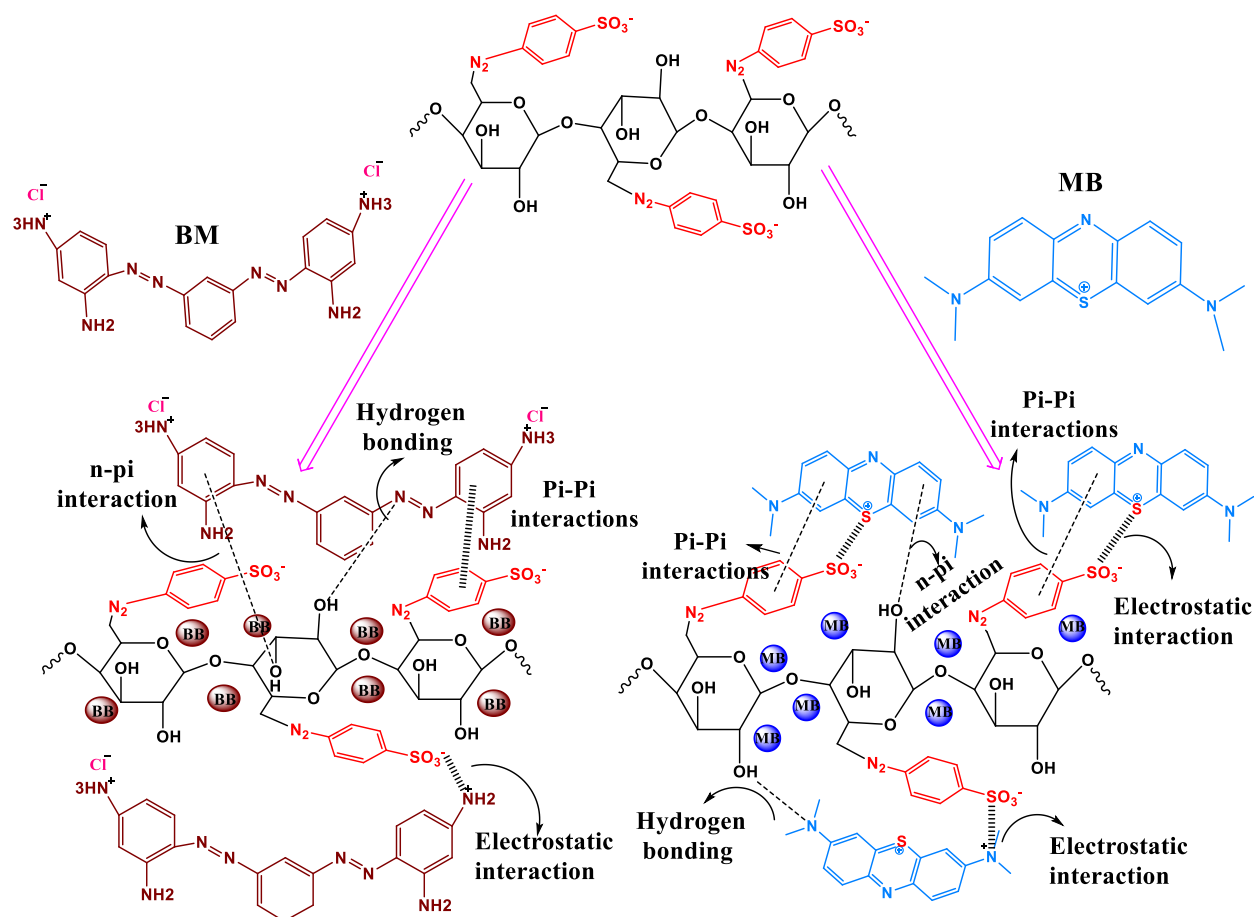
Figure 15. Plausible mechanism of adsorption of MB and BB onto SCB@SA biosorbent.

Dye	Adsorbent	$q_{e(mg/g)}$	Time, min	pH	Ref
MB	Phoenix tree's leaves	80.90	150	4.5	[33]
	Acer tree leaves	97.07	15	6	[34]
	Elaeis guineensis leaves	103.00	50	6	[35]
	Typha angustifolia leaves	106.75	60	10	[36]
	Banana leaves	109.90	280	7	[37]
	Cocos nucifera leaf	112.35	25	7	[38]
	Platanus orientalis leaf powder	114.90	70	12	[39]
	Pine Tree leaves	126.58	100	9.2	[40]
	Poplar leaf	135.40	240	7	[41]
	Porous alginate-based polyHIPE	66.87	60	8	[28]
	SCB@SA biosorbent	136.99	120	7	This work
BB	MCM-48	158.7301	120	7	[42]
	Citric acid modified pea peel	5.37	60	7	[43]
	Blast furnace sludge	8.2	180	7	[44]
	ZSAC	35.84	20	5	[45]
	AC2/Fe/CuO	39.2156	15	5	[46]
	Activated sewage sludge	7.543	240	2	[47]
	MWCNTs	32.15	10	5	[48]
	SCB@SA biosorbent	166.67	120	7	This work

Table 4. Comparison of adsorption capacity of MB and BB onto SCB@SA biosorbent with previously reported studies.
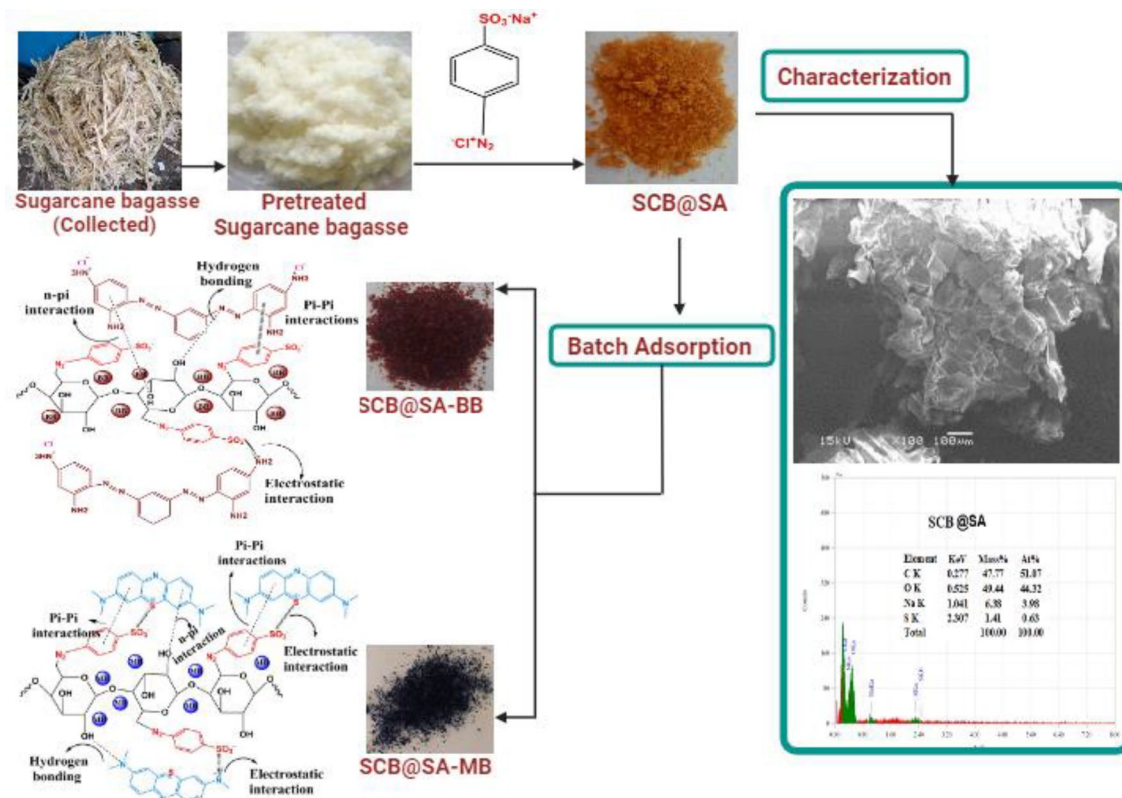
Figure 16. Synthesis and characterization of SCB@SA biosorbent and its use for MB and BB adsorption.

Data availability
All data generated or analyzed during this study are included in this published article.

References
1. Akl, M. A., Mostafa, A. G., Abdelaal, M. Y. & Nour, M. A. K. Surfactant supported chitosan for efficient removal of Cr (VI) and anionic food stuff dyes from aquatic solutions. *Sci. Rep.* **13**(1), 15786. https://doi.org/10.1038/s41598-023-43034-9 (2023).
2. Mostafa, A. G., Abd El-Hamid, A. I. & Akl, M. A. Surfactant-supported organoclay for removal of anionic food dyes in batch and column modes: Adsorption characteristics and mechanism study. *Appl. Water Sci.* **13**(8), 163. https://doi.org/10.1007/s13201-023-01959-6 (2023).
3. Yang, Z. *et al.* Au/Boron organic frameworks for efficient removal and degradation of azo dye pollutants. *Colloids Surf. A Physicochem. Eng. Asp.* **646**, 128884. https://doi.org/10.1016/j.colsurfa.2022.128884 (2022).
4. Akl, M. A., El-Mahdy, N., Al-Awadhi, M. M. & Mostafa, A. Cationic organo-montmorillonite for efficient concomitant removal of anionic dyes in single and multi-components' solutions: Adsorption characteristics and mechanism study. *Egypt. J. Chem.* https://doi.org/10.21608/ejchem.2023.210347.7962 (2023).
5. Shin, J. H. *et al.* Rapid and efficient removal of anionic dye in water using a chitosan-coated iron oxide-immobilized polyvinylidene fluoride membrane. *ACS Omega* **7**(10), 8759–8766. https://doi.org/10.1021/acsomega.1c06991 (2022).
6. Patel, H., Routoula, E. & Patwardhan, S. V. Decontamination of anthraquinone dyes polluted water using bioinspired silica as a sustainable sorbent. *Silicon* https://doi.org/10.1007/s12633-020-00851-1 (2022).
7. Alnoman, R. B., Aljohani, M. S., Alharbi, H. Y., Bukhari, A. A. H. & Monier, M. Development and assessment of isatin hydrazone-functionalized/ion-imprinted cellulose adsorbent for gadolinium (III) removal. *Int. J. Biol. Macromol.* **256**, 128186. https://doi.org/10.1016/j.ijbiomac.2023.128186 (2024).
8. Elsayed, N. H., Monier, M., Alatawi, R. A. & Al-Anazi, M. Design of ion-imprinted cellulose-based microspheres for selective recovery of uranyl ions. *Carbohyd. Polym.* **313**, 120873. https://doi.org/10.1016/j.carbpol.2023.120873 (2023).
9. Elsayed, N. H. *et al.* Selective removal of uranyl ions using ion-imprinted amino-phenolic functionalized chitosan. *Int. J. Biol. Macromol.* **237**, 124073. https://doi.org/10.1016/j.ijbiomac.2023.124073 (2023).
10. Yang, S. T. *et al.* Removal of methylene blue from aqueous solution by graphene oxide. *J. Colloid Interface Sci.* **359**(1), 24–29. https://doi.org/10.1016/j.jcis.2011.02.064 (2011).
11. Oladipo, A. A. & Gazi, M. Enhanced removal of crystal violet by low cost alginate/acid activated bentonite composite beads: Optimization and modelling using non-linear regression technique. *J. Water Process Eng.* **2**, 43–52. https://doi.org/10.1016/j.jwpe.2014.04.007 (2014).
12. Oladipo, A. A. & Ifebajo, A. O. Highly efficient magnetic chicken bone biochar for removal of tetracycline and fluorescent dye from wastewater: Two-stage adsorber analysis. *J. Environ. Manag.* **209**, 9–16. https://doi.org/10.1016/j.jenvman.2017.12.030 (2018).
13. Bhujbal, S. K. *et al.* Biotechnological potential of rumen microbiota for sustainable bioconversion of lignocellulosic waste to biofuels and value-added products. *Sci. Total Environ.* **814**, 152773. https://doi.org/10.1016/j.scitotenv.2021.152773 (2022).
14. Lin, Q. *et al.* Effectively removal of cationic and anionic dyes by pH-sensitive amphoteric adsorbent derived from agricultural waste-wheat straw. *J. Taiwan Inst. Chem. Eng.* **76**, 65–72. https://doi.org/10.1016/j.jtice.2017.04.010 (2017).

15. Zhou, T. *et al.* Effective adsorption of light green anionic dye from solution by CPB modified peanut in column mode. *J. Mol. Liq.* **211**, 909–914. https://doi.org/10.1016/j.molliq.2015.08.018 (2015).
16. Lyu, W., Yu, M., Feng, J. & Yan, W. Highly crystalline polyaniline nanofibers coating with low-cost biomass for easy separation and high efficient removal of anionic dye ARG from aqueous solution. *Appl. Surf. Sci.* **458**, 413–424. https://doi.org/10.1016/j.apsusc.2018.07.074 (2018).
17. Velinov, N. *et al.* Wood residue reuse for a synthesis of lignocellulosic biosorbent: characterization and application for simultaneous removal of copper (II), Reactive Blue 19 and cyprodinil from water. *Wood Sci. Technol.* **53**, 619–647. https://doi.org/10.1007/s00226-019-01093-0 (2019).
18. Ghosh, S. K. & Bandyopadhyay, A. Adsorption of methylene blue onto citric acid treated carbonized bamboo leaves powder: Equilibrium, kinetics, thermodynamics analyses. *J. Mol. Liq.* **248**, 413–424. https://doi.org/10.1016/j.molliq.2017.10.086 (2017).
19. Bello, O. S., Lasisi, B. M., Adigun, O. J. & Ephraim, V. Scavenging Rhodamine B dye using *Moringa oleifera* seed pod. *Chem. Spec. Bioavail.* **29**(1), 120–134 https://doi.org/10.1080/09542299.2017.1356694 (2017)
20. Halili, J., Salihu, F. & Berisha, A. R. Covalent attachment of phenyl and carboxyphenyl layers derived from diazonium salts onto activated charcoal for the adsorption of pesticides. *Macedonian J. Chem. Chem. Eng.* **37**(1), 71–78 https://doi.org/10.20450/mjcce.2018.1442 (2018).
21. Abd-Elhamid, A. I., Abu Elgoud, E. M. & Aly, H. F. Sugarcane bagasse decorated by metal (Fe³⁺/Cu²⁺) ferrocyanide for effective removal of cesium from aqueous solutions. *J. Water Process Eng.* **57**, 104641 https://doi.org/10.1016/j.jwpe.2023.104641 (2024).
22. Akl, M. A., Mostafa, A. G., Al-Awadhi, M., Al-Harwi, W. S. & El-Zeny, A. S. Zinc chloride activated carbon derived from date pits for efficient biosorption of brilliant green: Adsorption characteristics and mechanism study. *Appl. Water Sci.* **13**(12), 226 https://doi.org/10.1007/s13201-023-02034-w (2023).
23. Mostafa, A. G., Gaith, E. A. & Akl, M. A. Aminothiol supported dialdehyde cellulose for efficient and selective removal of Hg (II) from aquatic solutions. *Sci. Rep.* https://doi.org/10.1038/s41598-023-46082-3 (2023).
24. Faroughi, N. H., Hazeri, N., Rezaie, K. M. & Maghsoodlou, M. T. Preparation and characterization of MNPs–PhSO 3 H as a heterogeneous catalyst for the synthesis of benzo [b] pyran and pyrano [3, 2-c] chromenes. *Res. Chem. Intermediates* **46**, 1685–1704. https://doi.org/10.1007/s11164-019-04056-z (2020).
25. Lei, Y. *et al.* Facile preparation of sulfonic groups functionalized Mxenes for efficient removal of methylene blue. *Ceram. Int.* **45**(14), 17653–17661. https://doi.org/10.1016/j.ceramint.2019.05.331 (2019).
26. Hu, X. J. *et al.* Removal of Cu (II) ions from aqueous solution using sulfonated magnetic graphene oxide composite. *Sep. Purif. Technol.* **108**, 189–195. https://doi.org/10.1016/j.seppur.2013.02.011 (2013).
27. Prema, P. *et al.* Hexavalent chromium removal from aqueous solutions using biogenic iron nanoparticles: Kinetics and equilibrium study. *Environ. Res.* **205**, 112477. https://doi.org/10.1016/j.envres.2021.112477 (2022).
28. Ansari, H., Oladipo, A. A. & Gaz, M. Alginate-based porous polyHIPE for removal of single and multi-dye mixtures: Competitive isotherm and molecular docking studies. *Int. J. Biol. Macromol.* **246**, 125736. https://doi.org/10.1016/j.ijbiomac.2023.125736 (2023).
29. Oladipo, A. A., Ahaka, E. O. & Gazi, M. High adsorptive potential of calcined magnetic biochar derived from banana peels for Cu²⁺, Hg²⁺, and Zn²⁺ ions removal in single and ternary systems. *Environ. Sci. Pollut. Res.* **26**(31), 31887–31899. https://doi.org/10.1007/s11356-019-06321-5 (2019).
30. Liu, M., Chen, C., Hu, J., Wu, X. & Wang, X. Synthesis of magnetite/graphene oxide composite and application for cobalt (II) removal. *J. Phys. Chem. C* **115**(51), 25234–25240. https://doi.org/10.1021/jp208575m (2011).
31. El Shahawy, A., Mubarak, M. F., El Shafie, M. & Abdulla, H. M. Fe (III) and Cr (VI) ions' removal using AgNPs/GO/chitosan nanocomposite as an adsorbent for wastewater treatment. *RSC Adv.* **12**(27), 17065–17084. https://doi.org/10.1039/D2RA01612E (2022).
32. Aksu, Z. & Kutsal, T. A bioseparation process for removing lead (II) ions from waste water by using *C. vulgaris*. *J. Chem. Technol. Biotechnol.* **52**(1), 109–118. https://doi.org/10.1002/jctb.280520108 (1991).
33. Han, R. *et al.* Biosorption of methylene blue from aqueous solution by fallen phoenix tree's leaves. *J. Hazard. Mater.* **141**(1), 156–162. https://doi.org/10.1016/j.jhazmat.2006.06.107 (2007).
34. Zolgharnein, J. & Bagtash, M. Hybrid central composite design optimization for removal of Methylene blue by Acer tree leaves: Characterization of adsorption. *Desalin. Water Treat.* **54**(9), 2601–2610. https://doi.org/10.1080/19443994.2014.901192 (2015).
35. Setiabudi, H. D., Jusoh, R., Suhaimi, S. F. R. M. & Masrur, S. F. Adsorption of methylene blue onto oil palm (*Elaeis guineensis*) leaves: Process optimization, isotherm, kinetics and thermodynamic studies. *J. Taiwan Inst. Chem. Eng.* **63**, 363–370. https://doi.org/10.1016/j.jtice.2016.03.035 (2016).
36. Boumaza, S. *et al.* Application of *Typha angustifolia* (L.) dead leaves waste as biomaterial for the removal of cationic dye from aqueous solution. *Int. J. Environ. Res.* **12**, 561–573. https://doi.org/10.1007/s41742-018-0111-1 (2018).
37. Krishni, R. R., Foo, K. Y. & Hameed, B. H. Adsorptive removal of methylene blue using the natural adsorbent-banana leaves. *Desalin. Water Treat.* **52**(31–33), 6104–6112. https://doi.org/10.1080/19443994.2013.815687 (2014).
38. Jawad, A. H. *et al.* Adsorption of methylene blue onto coconut (*Cocos nucifera*) leaf: Optimization, isotherm and kinetic studies. *Desalin. Water Treat.* **57**(19), 8839–8853. https://doi.org/10.1080/19443994.2015.1026282 (2016).
39. Peydayesh, M. & Rahbar-Kelishami, A. Adsorption of methylene blue onto *Platanus orientalis* leaf powder: Kinetic, equilibrium and thermodynamic studies. *J. Indus. Eng. Chem.* **21**, 1014–1019. https://doi.org/10.1016/j.jiec.2014.05.010 (2015).
40. Yagub, M. T., Sen, T. K. & Ang, H. M. Equilibrium, kinetics, and thermodynamics of methylene blue adsorption by pine tree leaves. *Water Air Soil Pollut.* **223**, 5267–5282. https://doi.org/10.1007/s11270-012-1277-3 (2012).
41. Han, X., Niu, X. & Ma, X. Adsorption characteristics of methylene blue on poplar leaf in batch mode: Equilibrium, kinetics and thermodynamics. *Korean J. Chem. Eng.* **29**, 494–502. https://doi.org/10.1007/s11814-011-0211-5 (2012).
42. Zakir, M. *et al.* Adsorption of bismarck brown R dyes using mesoporous silica MCM-48. *Indones. J. Chem. Res.* **10**(2), 117–124. https://doi.org/10.30598/ijcr.2022.10-muh (2022).
43. Khan, T. A., Rahman, R. & Khan, E. A. Decolorization of bismarck brown R and crystal violet in liquid phase using modified pea peels: Non-linear isotherm and kinetics modeling. *Model. Earth Syst. Environ.* **2**, 1–11. https://doi.org/10.1007/s40808-016-0195-6 (2016).
44. Bhatnagar. A. & Jain, A. K. A comparative adsorption study with different industrial wastes as adsorbents for the removal of cationic dyes from water. *J. Colloid Interface Sci.* **281**(1), 49–55 https://doi.org/10.1016/j.jcis.2004.08.076 (2005)
45. Vatankhah, G. & Koohmareh, H. Enhanced removal of bismark brown (BB) dye from aqueous solutions using activated carbon from raw Ziziphusspina-christi (ZSAC) equilibrium, thermodynamic and kinetics. *J. Phys. Theor. Chem.* **14**(3), 237–249 (2017).
46. Jabbar, R. K. & Atiyah, A. J. Removal of bismarck brown G dye over composites of metalized copper oxide nanoparticles with nitrogen and activated carbons. *J. Phys. Conf. Ser.* (IOP Publishing) **1999**(1), 012011 https://doi.org/10.1088/1742-6596/1999/1/012011 (2021).
47. Ali, S. H. & Jassim, T. E. Thermodynamics and kinetic study of bismarck brown R dye adsorption from aqueous solution using sewage sludge. *Basrah J. Sci.* **38**(2), 248–270 (2020).
48. Kamil, A. M., Abdalrazak, F. H., Halbus, A. F. & Hussein, F. H. Adsorption of Bismarck brown R dye onto multiwall carbon nanotubes. *J. Environ. Anal. Chem.* **1**(104), 2. https://doi.org/10.4172/2380-2391.1000104 (2014).

Author contributions

A.I. Abd-Elhamid: Conceptualization, Methodology, Investigation, Writing-original draft, review. A. G. Mostafa : Methodology, investigation, writing-original draft, review. A. A. Nayl : Conceptualization, Methodology, Investigation, Writing-original draft, review. M. A. Kl : Conceptualization, Methodology, Investigation, Writing-original draft, review.

Competing interests

The authors declare no competing interests.

Additional information

Correspondence and requests for materials should be addressed to M.A.A.

Reprints and permissions information is available at www.nature.com/reprints.

Publisher's note Springer Nature remains neutral with regard to jurisdictional claims in published maps and institutional affiliations.